

**DAHLGREN DIVISION
NAVAL SURFACE WARFARE CENTER**

Dahlgren, Virginia 22448-5100



NSWCDD/TR-17/463

**MITIGATING BLAST AND SHOCK WITH ADVANCED
MATERIALS**

**BY SUSAN BARTYCZAK
EMMA DOHMEIER
LAUREN EDGERTON
WILLIS MOCK**

WEAPONS CONTROL AND INTEGRATION DEPARTMENT

JUNE 2018

DISTRIBUTION STATEMENT A: Approved for public release. Distribution is unlimited.

REPORT DOCUMENTATION PAGE			<i>Form Approved</i> <i>OMB No. 0704-0188</i>	
Public reporting burden for this collection of information is estimated to average 1 hour per response, including the time for reviewing instructions, searching existing data sources, gathering and maintaining the data needed, and completing and reviewing this collection of information. Send comments regarding this burden estimate or any other aspect of this collection of information, including suggestions for reducing this burden to Department of Defense, Washington Headquarters Services, Directorate for Information Operations and Reports (0704-0188), 1215 Jefferson Davis Highway, Suite 1204, Arlington, VA 22202-4302. Respondents should be aware that notwithstanding any other provision of law, no person shall be subject to any penalty for failing to comply with a collection of information if it does not display a currently valid OMB control number. PLEASE DO NOT RETURN YOUR FORM TO THE ABOVE ADDRESS.				
1. REPORT DATE (DD-MM-YYYY) 31 March 2018		2. REPORT TYPE Technical		3. DATES COVERED (From - To) 1 March–31 March 2018
4. TITLE AND SUBTITLE Mitigating Blast and Shock Using Advanced Materials			5a. CONTRACT NUMBER	
			5b. GRANT NUMBER	
			5c. PROGRAM ELEMENT NUMBER	
6. AUTHOR(S) Susan Bartyczak, Emma Dohmeier, Lauren Edgerton, Willis Mock			5d. PROJECT NUMBER	
			5e. TASK NUMBER	
			5f. WORK UNIT NUMBER	
7. PERFORMING ORGANIZATION NAME(S) AND ADDRESS(ES) AND ADDRESS(ES) Naval Surface Warfare Center, Dahlgren Division (Code H32) Dahlgren, VA 22448-5100			8. PERFORMING ORGANIZATION REPORT NUMBER NSWCDD/TR-17/463	
9. SPONSORING / MONITORING AGENCY NAME(S) AND ADDRESS(ES)			10. SPONSOR/MONITOR'S ACRONYM(S)	
			11. SPONSOR/MONITOR'S REPORT NUMBER(S)	
12. DISTRIBUTION / AVAILABILITY STATEMENT Approved for public release. Distribution is unlimited..				
13. SUPPLEMENTARY NOTES				
14. ABSTRACT Naval Surface Warfare Center, Dahlgren Division, is collaborating with Naval Surface Warfare Center, Carderock Division, and Naval Undersea Warfare Center, Division Newport, to produce layered polyurea/woven crimp graded composite panels optimized for blast and fragment impact protection. The intent is to develop blast and impact resistant elastomeric coatings and woven fabric-reinforced polymer composites for use in numerous structural and survivability applications as well as applications where improved lightweight blast and impact protection is a necessity. This report documents the NSWCDD light gas gun experimental portion of this effort.				
15. SUBJECT TERMS gas gun...WFRP composites...Hugoniot reserve ballistics...equation of state				
16. SECURITY CLASSIFICATION OF:			17. LIMITATION OF ABSTRACT SAR	18. NUMBER OF PAGES 32
a. REPORT UNCLASSIFIED	b. ABSTRACT UNCLASSIFIED	c. THIS PAGE UNCLASSIFIED		
			19b. TELEPHONE NUMBER (include area code) 540.653.8687	

(THIS PAGE INTENTIONALLY LEFT BLANK)

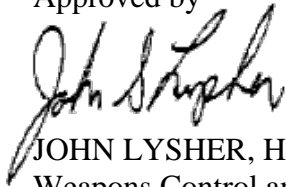
FOREWORD

The Naval Surface Warfare Center, Dahlgren Division (NSWCDD), is collaborating with Naval Surface Warfare Center, Carderock Division (NSWCCD), and Naval Undersea Warfare Center, Division Newport (NUWC DIVNPT), to produce layered polyurea/woven crimp-graded composite panels optimized for blast and fragment impact protection. The intent was to develop blast and impact resistant elastomeric coatings and woven fabric-reinforced polymer composites for use in numerous structural and survivability applications as well as applications where improved lightweight blast and impact protection is a necessity. This report documents the NSWCDD light gas gun experimental portion of this effort.

This project was funded by the Naval Innovative Science and Engineering Program. The authors gratefully acknowledge James LeBlanc and Paul Cavallaro, NUWC DIVNPT; and Jeffrey Fedderly, Edward Balizer, and Jaime Santiago, NSWCCD; for providing materials and helpful discussions regarding experimental results.

This document has been reviewed by Jacquelyn Porter, Head, Lethality and Effectiveness Branch; and Steve Collignon, Head, Missile Systems Integration and Weapons Effectiveness Division.

Approved by



JOHN LYSHER, Head
Weapons Control and Integration Department

(THIS PAGE INTENTIONALLY LEFT BLANK)

CONTENTS

Section	Page
Introduction	1
Shock Physics Facility	1
Phase 1	2
Materials	2
Planar Blast Wave Experiments	2
Experimental Setup	2
Results and Discussion	4
Flyer Plate Impact Experiments.....	9
Experimental Setup	9
Results and Discussion	10
Phase 1 Conclusion.....	13
Blast Wave Experiments	13
Flyer Plate Impact Experiments	14
Phase 2	14
Materials	14
Experimental Setup	15
Results and Discussion	17
Phase 2 Conclusions	19

LIST OF ILLUSTRATIONS

Figure	Page
Figure 1: NSWCDD Shock Facility	1
Figure 2: Muzzle Adapter and Target Assembly	3
Figure 3: Exploded View of Muzzle Adapter and Removable Muzzle Adapter Flange	3
Figure 4: Schematic of Target Assembly	4
Figure 5: Exploded View of Target Assembly Attached to Muzzle Adapter	4
Figure 6: 6061-T6 Al Target Calibration Experiment at 1 bar Air Blast Pressure	5
Figure 7: PVDF Gauge Data for the 9.06mm-thick P650 Polyurea Experiment at 2 bar Incident Air Blast Pressure ..6	6
Figure 8: U-u Blast Wave Properties for Polymers	7
Figure 9: Left, σ - u and σ - ε , right, Blast Wave Properties for Polymers.....	7
Figure 10: Schematic of Impedance Matching Technique for Stress Attenuation Determination.....	8
Figure 11: Blast Wave Amplitude versus Polymer Thickness.....	9
Figure 12: Flyer Plate Experiment Setup Cutaway.....	10
Figure 13: Flyer Plate Experiment Setup.....	10
Figure 14: Manganin Gauge Results for Polyurea P250/1000 for Cu Disc Impact at 0.762mm/ μ s	11
Figure 15: (a) P250/1000 U - u Shock Properties (b) Dragonshield-BC U - u Shock Properties	12
Figure 16: (a) P250/1000 σ - u Shock Properties (b) Dragonshield-BC σ - u Shock Properties	12
Figure 17: Kevlar Weave Styles	14
Figure 18: Target and Sabot Assembly Cutaway	17
Figure 19: Plain Weave Kevlar below Penetration Threshold Result.....	18
Figure 20: Twill Weave Kevlar below Penetration Threshold Result	19
Figure 21: Hybrid Weave Kevlar below Penetration Threshold Result	19
Figure 22: Hybrid Weave Kevlar above Penetration Threshold Result.....	19

LIST OF TABLES

Table	Page
Table 1: Polymer Dimensions	5
Table 2: Blast Attenuation Results	8
Table 3: Attenuation Coefficients	9
Table 4: Polyurea P250/1000 Principal Hugoniot Experimental Results	13
Table 5: Dragonshield-BC Principal Hugoniot Experimental Results	13
Table 6: Nominal Mechanical Properties of Kevlar KM2 Plus Yarns	15
Table 7: Kevlar KM2 Plus Fabric Weave Styles and Properties	15
Table 8: Kevlar Sample Dimensions	16
Table 9: Kevlar Penetration Threshold Results	18

GLOSSARY

NSWCDD	Naval Surface Warfare Center, Dahlgren Division
NSWCCD	Naval Surface Warfare Center, Carderock Division
NUWC DIVNPT	Naval Undersea Warfare Center Division Newport
OFHC	oxygen-free high-thermal conductivity
PVDF	polyvinylidene fluoride
CG	crimp gradient

Only U.S. Navy- or NSWCDD-released images are used in this report unless otherwise noted.

“Versalink®” and “Air Products®” are registered to Air Products and Chemicals, Inc. (PRIVATE COMPANY)

“Dow®™” and “Isonate™” are trademarks of The Dow Chemical Company

“Dragonshield-BC®” is a registered trademark of Specialty Products, Inc. (CORPORATION Alaska)

“Kevlar®”, “KM2®”, “Mylar®” are registered to and “DuPont™” is a trademark of E. I. du Pont de Nemours and Company, Inc. (CORPORATION Delaware)

“PCB®” is registered to PCB Piezotronics, Inc.

“Lexan®” is a registered trademark of Sabic Global Technologies B.V. (BESTOLEN VENNOOTSCHAP Netherlands)

“Parker®” is registered to and “Parker-Hannifin Corp.™” is a trademark of Parker Intangibles LLC (LIMITED LIABILITY COMPANY Delaware)

“Torr Seal®” is registered to Kurt J. Lesker Company® (CORPORATION Pennsylvania)

“PVDF Stress Gauge Model Number PVF₂-11-.125-EK” and “Manganin Gauge Part MN4-50-EFEP” are products of Dynasen, Inc.; no other information found.

“Dapco®” is registered to and DAPCOND T A NORDCO COMPANY™ is a trademark of Nordco Inc. (CORPORATION Delaware)

“EPO-TEK®” 301 is registered to Epoxy Technology Inc. (CORPORATION Massachusetts)

“Core Molding Technologies, Inc.” is the parent organization of “Core Composites Corporation”; no other information found.

THIS PAGE INTENTIONALLY LEFT BLANK

INTRODUCTION

The Naval Surface Warfare Center, Dahlgren Division (NSWCDD), in collaboration with Naval Surface Warfare Center, Carderock Division (NSWCDD), and Naval Undersea Warfare Center, Division Newport (NUWC DIVNPT); conducted experimental and analysis research to produce layered polyurea/woven crimp-graded composite panels optimized for blast and fragment impact protection. NSWCDD was responsible for evaluating the dynamic response of selected NUWC DIVNPT- and NSWCDD-provided composite and viscoelastic polymer materials. The total effort spanned fiscal years 2016–2017 and was divided into two phases. Phase 1 consisted of a series of blast and shock impact experiments to determine dynamic material parameters for four viscoelastic polymer materials: P1000, P650, P250/1000, and Specialty Products, Inc.'s Dragonshield-BC™. Phase 2 consisted of a series of reverse ballistic impact experiments on DuPont™ Kevlar® KM2®/fiber-woven composites to evaluate the effect of weave style on penetration threshold. NUWC DIVNPT and NSWCDD will use the results to develop new hybrid composites for blast and fragment impact protection.

SHOCK PHYSICS FACILITY

NSWCDD's Shock Physics Facility, shown in Figure 1, consists of a single stage 40mm bore gas gun with associated hardware and electronics that uses helium or nitrogen gas to accelerate objects to speeds of 60–975 m/s. The facility provides a multipurpose experimental capability used for a variety of applications including characterizing and optimizing materials and components that must perform in intense mechanical impulsive environments such as projectile, armor, and explosive ordnance applications; shockwave equation-of-state measurements on materials (for computational design and simulation); and precision impacts over a wide range of impact speeds into full-scale target configurations to measure deformation, penetration, and reactive energy release [1].

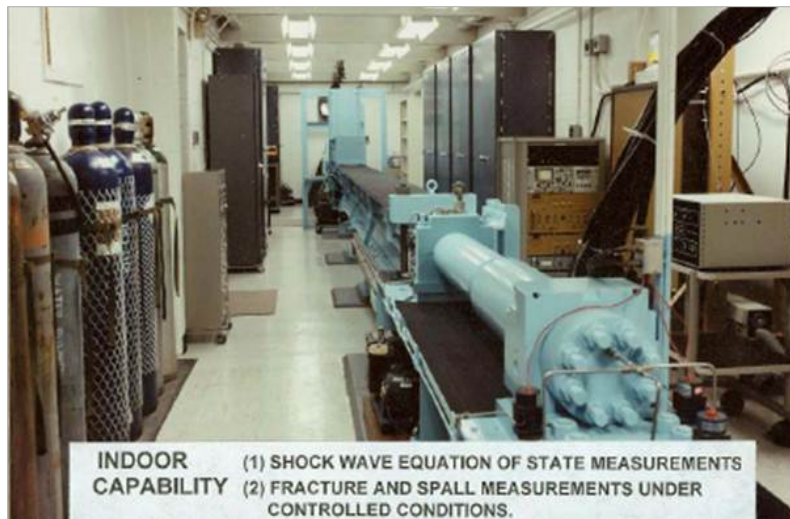


Figure 1: NSWCDD Shock Facility

This facility has been used for Navy research and development and fleet-support programs since 1971. Technologies investigated include dynamic fracture and fragmentation of projectile and missile warhead materials [2], barrier penetration by warhead fragments [3], effects of fragment impacts on weapon subsystems [4], impact fracture of composite materials [3], ship hull protection and/or defeat [5], impact shock-induced energy release from reactive materials

[6], [7], [8], and impact shock generation of high voltage pulse power [9].

PHASE 1

Phase 1 of this effort consisted of two types of experiments: planar air blast wave and flyer plate impact experiments. The planar air blast wave experiments were used to determine dynamic material parameters for three viscoelastic polyureas P1000, P650, and P250/1000, as well as the commercial polymer Dragonshield-BC in the low bar blast wave region (1 bar = 14.504 psi). The flyer plate impact experiments were used to determine dynamic material parameters for P250/1000 and Dragonshield-BC in the kilobar stress region (1 kilobar = 14,504 psi). Flyer plate impact experiments for P1000 and P650 were not performed because results from a prior effort were leveraged [10].

Materials

Jeff Fedderly from NSWCCD fabricated polyureas P1000, P650, and P250/1000. The polymer was fabricated from amine and isocyanate materials obtained from Air Products and Chemicals, Inc. and The Dow Chemical Company, respectively. The diamines are Air Products® Versalink® P1000, P650, and P250 diamines, where 1000, 650, and 250 refer to the nominal molecular weight of the polytetramethyleneoxideglycol starting material for the diamine. The diamines consist of tetramethyleneoxide repeat units with terminated primary aromatic amine esters. The isocyanate, Dow's Isonate™ 143L, is a eutectic mixture of pure linear, symmetric p,p.-diphenylmethane diisocyanate (MDI) and a carbodiimide modified MDI triisocyanate. The triisocyanate component adds asymmetry to the structure to prevent hard domain crystallinity and provides higher functionality for modest crosslinking. The tetramethyleneoxide component serves as the polyurea's soft segment while the terminal aromatic amine and isocyanate components serve as the hard segment. The weight percent of hard segments for P1000, P650, and P250/1000 blend (2.25:1) is 36%, 47%, and 55% respectively [11].

Dragonshield-BC is a spray-applied polymer designed for blast mitigation and fragment/spall containment in military applications, including vehicle and structural protection. Its properties include ultrahigh tensile strength, moderate elongation, superior tensile modulus, excellent tear strength, and moderate hardness. Since Dragonshield-BC is a commercial product and the material is proprietary, the details of its makeup are unknown.

Planar Blast Wave Experiments

To evaluate polymers for air blast mitigation, a recently developed muzzle adapter and target assembly, designed for use with the NSWCDD light gas gun, was employed to generate planar air blast waves in the range of 0.5 to 2 bar for 2 ms duration [12]. The instrumented target assembly provided measurements of air blast wave amplitude and velocity as well as input and output stress and blast attenuation in the polymer material. Also, polymer longitudinal wave velocity and particle velocity were determined. The Sandia National Laboratories' shock physics hydrocode CTH¹ was used to simulate and make comparisons to some of the experiments.

Experimental Setup

Muzzle Adapter

The muzzle adapter was designed to allow the blast wave to expand to a 63.5 mm diameter

¹ Government-owned, export-controlled software

and reform into a planar wave through a straight section as shown in Figure 2. The muzzle adapter assembly consists of a 304.8 mm-long cylinder with a conical cavity and a removable flange shown in Figure 3. The parts are fabricated from 6061-T6 aluminum. The gun barrel sits in a recess in the non-removable end of the muzzle adapter, and this joint is sealed for blast pressure with an O-ring.

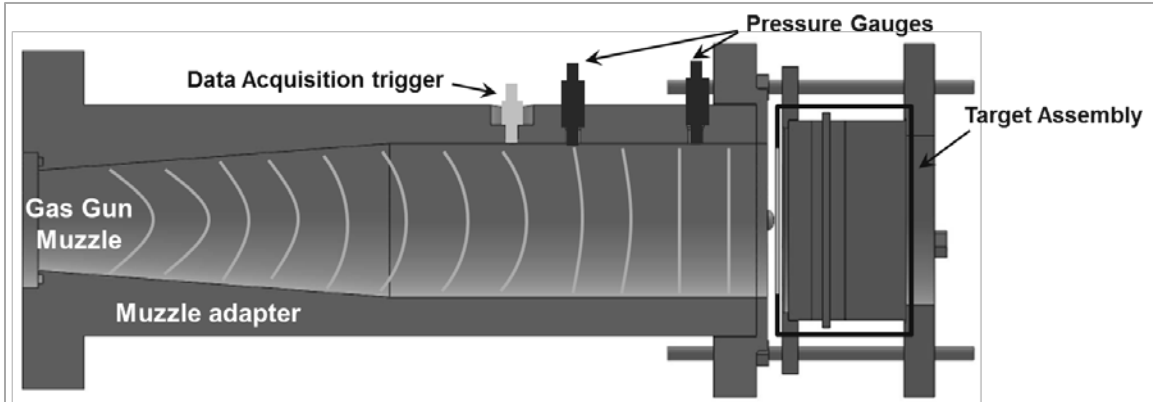


Figure 2: Muzzle Adapter and Target Assembly

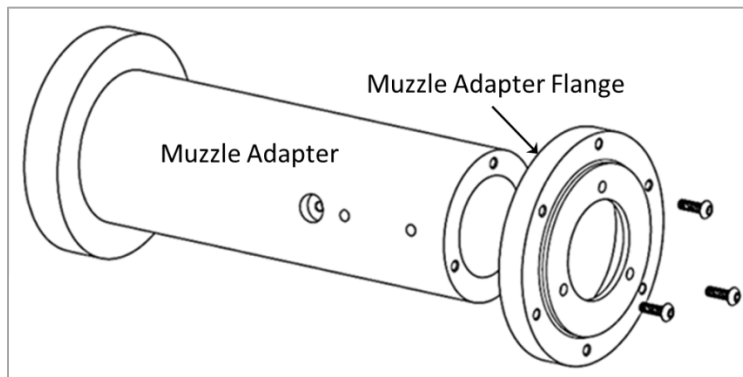


Figure 3: Exploded View of Muzzle Adapter and Removable Muzzle Adapter Flange

The muzzle adapter has a 146 mm long transition region with increasing inside diameter. In the transition region, the inside diameter of the muzzle adapter increases from 41.4 to 63.5 mm which continues for the remaining length of the adapter. The muzzle adapter contains three pressure gauges: a PCB Piezotronics, Inc. PCB® 132A31 gauge for triggering the recording oscilloscopes; and two PCB 113A31 gauges (PG1 and PG2) for measuring the blast wave velocity and pressure.² These gauges are located 101.6, 76.2, and 25.4 mm, respectively, from the target assembly end of the adapter.

Target Assembly

The target assembly consists of the sample sandwiched between front (blast wave side) and back gauge assemblies as shown in Figure 4. Each gauge assembly consists of a Dynasen, Inc. polyvinylidene fluoride (PVDF) PVF₂-11-.125-EK stress gauge sandwiched between two 82.6 mm diameter 6061-T6 aluminum discs. The PVDF active area is 3.2 mm on a side and 0.03 mm thick; the encapsulated gauge thickness is 0.1 mm. The aluminum disc thicknesses were selected to allow each PVDF stress gauge time to reach equilibrium before interface

² NSWCDD Blast Attenuation Mount patent application 15/701,774, submitted 12 September 2017.

reflections affected the measurements. The front gauge assembly comprises a 9.4 mm thick disc on the blast impact side—the PVDF1 stress gauge—and a 6.5 mm thick disc that interfaces with the front of the polymer. The back gauge assembly comprises a 6.0 mm thick disc that interfaces with the back of the polymer—the PVDF2 stress gauge—and a 25.4 mm thick disc. By using two stress gauges and the measured 6061-T6 aluminum elastic wave velocity and density, input and output stresses and wave velocity were determined for the polymer material. The same gauge assemblies were used for all the experiments in this low air blast stress range of 0.5–2 bar. Because of the large diameter (82.6 mm) of the aluminum discs compared to the PVDF gauge dimensions (3.2 mm on a side), the estimated time for side release waves to affect stress measurements is at least 6 μ s after air blast impact.

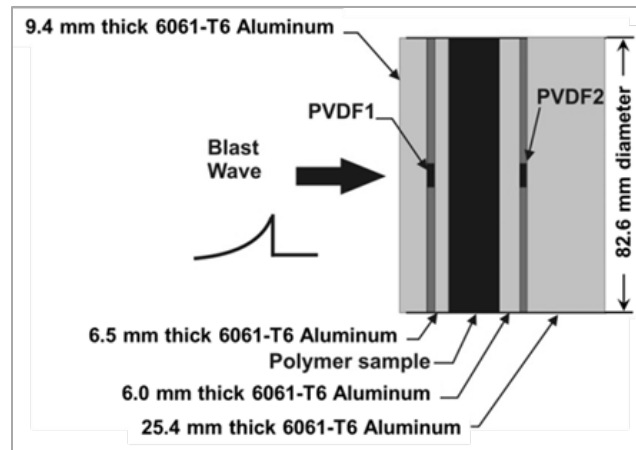


Figure 4: Schematic of Target Assembly

The target assembly is held together using a front plate, back plate, and three bolts as shown in Figure 5. The face of the target assembly is spaced 6.35 mm from the front face of the muzzle adapter flange to prevent barrel vibration from transmitting to the target assembly and to allow the blast pressure to escape after target impact.

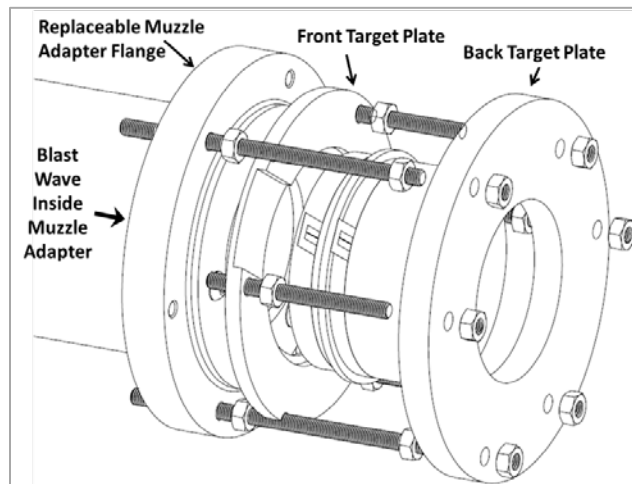


Figure 5: Exploded View of Target Assembly Attached to Muzzle Adapter

Results and Discussion

Several initial calibration experiments were performed with a 6061-T6 aluminum target. The two PVDF gauges recorded the same initial stress and rise time, within experimental error, for all

experiments, showing no attenuation in the aluminum sample. Figure 6 shows the result for a 1 bar blast wave. The darker curves are experimental results for the PVDF gauges, and the lighter curves are CTH simulations used to confirm that the gauge response represented the blast wave passing through the target and not electrical noise from the data acquisition system. The experimental initial pulse shape and amplitude for the two gauges are in close agreement until interface re-shockwaves affect the measurements. The CTH simulations are in good agreement with the gauge results through the first re-shock pulse for each gauge, about 3 μ s. The experimental calibration experiments were also used to calculate a 6.460 mm/ μ s longitudinal wave velocity for 6061-T6 aluminum, which was used for polymer data analysis and in the simulations. This measured value compares favorably with a literature value of 6.368 mm/ μ s [13].

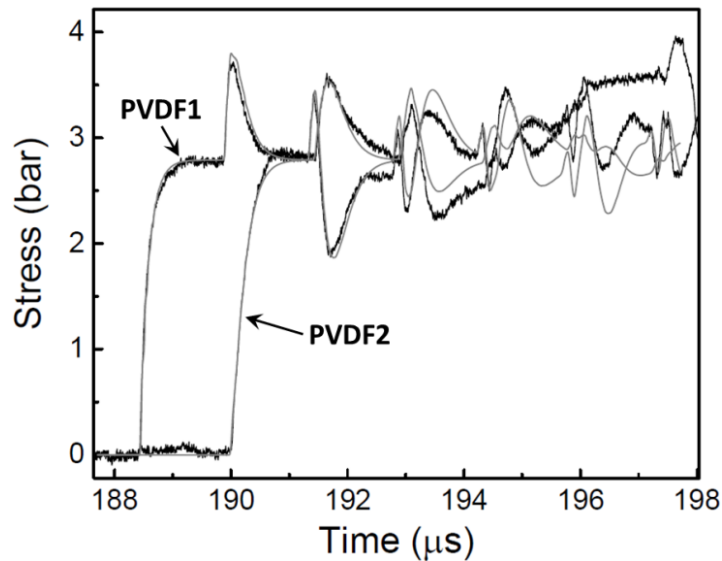


Figure 6: 6061-T6 Al Target Calibration Experiment at 1 bar Air Blast Pressure

Seven polymer targets were investigated (two thicknesses of each material except P250/1000, which was only available in one thickness). Each polymer target was evaluated at four incident air blast overpressures representing the environment of interest: nominally 0.5, 1, 1.5, and 2 bar. For P1000, P650, and Dragonshield-BC, blast wave properties were determined a function of polymer thickness. Table 1 lists each target's thickness and density.

Table 1: Polymer Dimensions

Polymer	Thickness (mm)	Density (g/cc)
P1000	3.33	1.105
P1000	9.88	1.105
P650	2.42	1.134
P650	9.06	1.145
P250/1000	6.35	1.166
Dragonshield-BC	3.86	0.938
Dragonshield-BC	7.16	0.964

Figure 7 shows PVDF stress data for one of the P650 experiments. The initial plateau in PVDF1 is taken as the input stress in the aluminum sandwich in front of the polymer. At the front aluminum-polymer interface, this wave is transmitted and reflected as a lower stress owing to the lower shock impedance polymer. At the back polymer-aluminum interface, the wave is

transmitted as a higher stress because of the higher aluminum shock impedance. The initial plateau in PVDF2 before the small reflected pulse appears is taken as the output stress in the back aluminum sandwich.

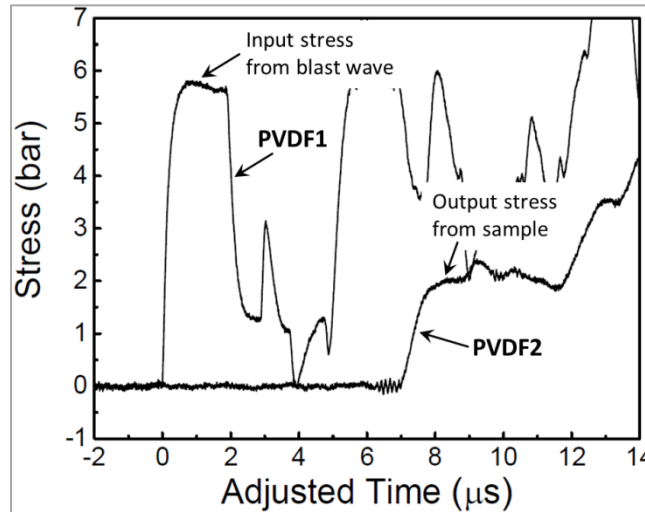


Figure 7: PVDF Gauge Data for the 9.06mm-thick P650 Polyurea Experiment at 2 bar Incident Air Blast Pressure

The polymer longitudinal wave velocity U was calculated using $U = d/(\Delta t - \Delta t_{Al} - \Delta t_G)$ where d is the measured polymer thickness and Δt is the blast wave transit time, which was taken as the time difference between the measured initial rise of the PVDF1 and PVDF2 signal responses. Δt_{Al} is the transit time through the two 6061-T6 aluminum discs in contact with the polymer, and was determined by dividing the thickness of the discs by the average measured 6.460mm/ μ s longitudinal wave velocity for 6061-T6 aluminum. Δt_G is the estimated transit time through a gauge package. The particle velocity u was calculated using $u = \sigma/(\rho_0 U)$ where σ and ρ_0 are the polymer input interface stress and density, respectively. σ is determined by impedance matching between the calculated polymer Rayleigh line and the aluminum elastic equation reflected about PVDF1.

Figure 8 illustrates the experimental polymer wave velocity for each experiment and the average $U-u$ curve. The curves are a linear least squares fit to the data and are of the standard form $U = C_0 + su$, where C_0 and s are equation of state parameters for the polymer. The C_0 values for P1000, P650, and P250/1000 are in excellent agreement with our measured ultrasonic longitudinal 1650, 1840, and 1960 m/s wave velocities, respectively, based on personal communication with J. Liu.³ As expected, the slope of the calculated $U-u$ curves is nearly zero in the measured polymer stress range of 0.3 to 1.5 bar. Also, the measured wave velocities are not significantly affected by different polymer thicknesses.

³ Polyurea 1000 ultrasonic longitudinal and shear wave velocities are 1.66 and 0.96 mm/ μ s, respectively. The calculated bulk sound speed and Poisson's ratio are 1.24 mm/ μ s and 0.249, respectively. The authors measured ultrasonic longitudinal velocities of P1000, P650, and P250/1000 of 1.65, 1.84, and 1.96 mm/ μ s wave, respectively, using a 5 MHz Dapco® longitudinal wave transducer.

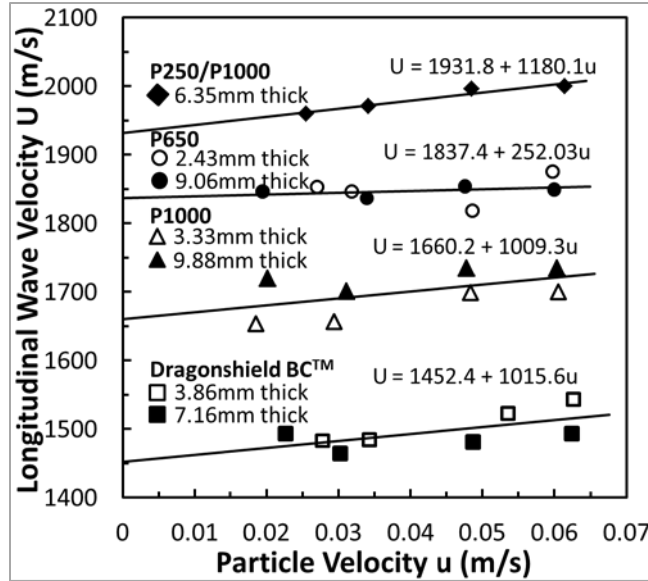


Figure 8: U-u Blast Wave Properties for Polymers

The calculated stress-particle velocity and stress-strain points for each experiment are shown in Figure 9, left and right, respectively. The curve fits for each polymer were determined by substituting $U = C_0 + su$ from Figure 8 into $\sigma = \rho_0 Uu$ for Figure 9 (left) and $\sigma = \rho_0 U^2 \epsilon$ for Figure 9 (right), where $\epsilon = u/U$ is the engineering strain. The resulting curves are $\sigma = \rho_0 C_0 u + \rho_0 s u^2$ and $\sigma = \rho_0 C_0^2 \epsilon / (1 - s \epsilon)^2$, respectively. For these calculations, the average densities for P1000, P650, and Dragonshield-BC were used.

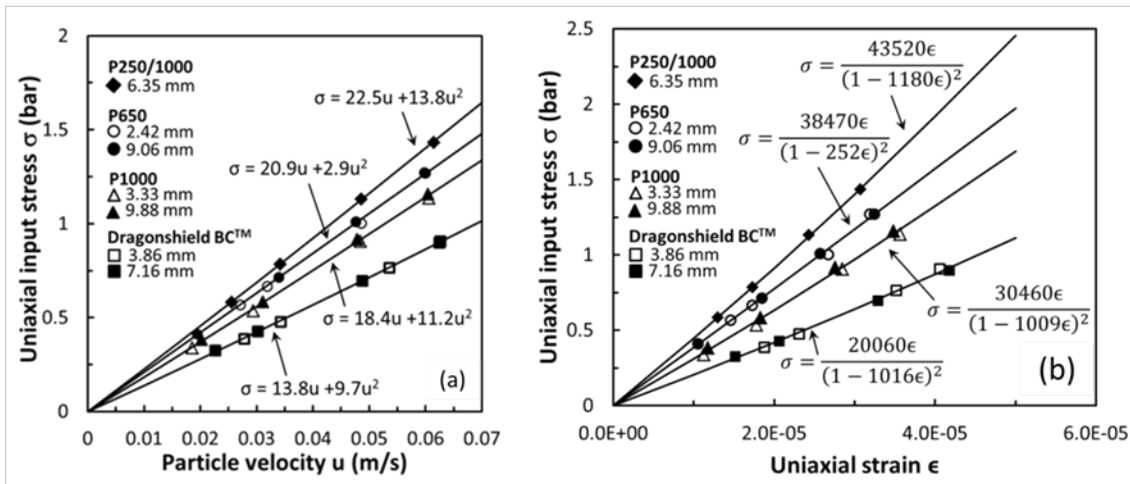


Figure 9: Left, $\sigma-u$ and $\sigma-\epsilon$, right, Blast Wave Properties for Polymers

Polymer stress attenuation calculations were performed analytically using the measured $\sigma-u$ properties for the polymer from Figure 9 (left) and 6061-T6 aluminum using wave impedance matching techniques.

Figure 10 illustrates this procedure. The polymer input stress is determined from the intersection of the polymer Rayleigh line and the aluminum elastic equation reflected about PVDF1. The polymer output stress is determined by reflecting the polymer $\sigma-u$ equation through the PVDF2 aluminum stress as illustrated in Figure 10. The intersection of the reflected and

forward-facing polymer σ - u equations determines the polymer output stress. This procedure was performed for each experiment.

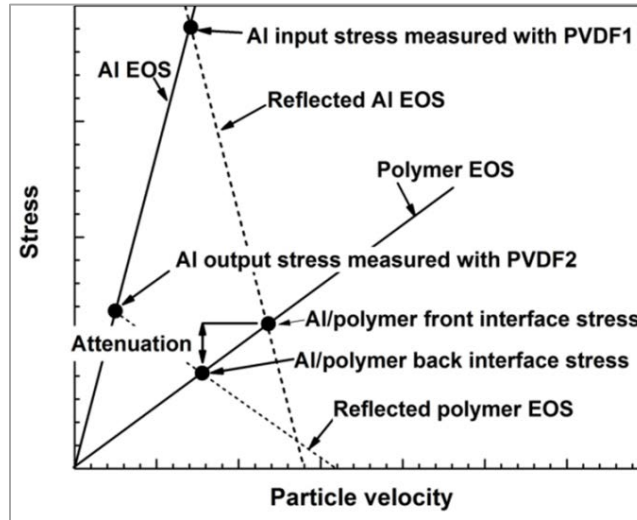


Figure 10: Schematic of Impedance Matching Technique for Stress Attenuation Determination

Table 2 lists average stress attenuation for each polymer thickness. As expected, the attenuation increases with polymer thickness but not in a linear manner. For example, for P1000 and P650, the attenuation doubles for a tripling of the polymer thickness. Dragonshield-BC shows significantly more attenuation than the other polymers.

Table 2: Blast Attenuation Results

Polymer	Thickness (mm)	Average Blast Attenuation for Four Blast Pressures (%)	Average Blast Attenuation per mm Thickness
P1000	3.33	6	1.8
P1000	9.88	10	1.1
P650	2.42	5	2.3
P650	9.06	10	1.1
P250/1000	6.35	7	1.1
Dragonshield-BC	3.86	24	6.2
Dragonshield-BC	7.17	37	5.2

It is possible to estimate an attenuation coefficient for the polymer materials. Earlier work showed that an initial sound wave amplitude A_0 in a solid decreases exponentially to amplitude A after propagating a distance x according to $A = A_0 \exp(-\alpha x)$, where α is an amplitude attenuation coefficient per unit distance [14]. We applied this procedure to our low-amplitude blast wave experiments even though acoustic waves involve infinitesimal pressure and particle velocity changes [15]. Attenuation is mainly caused by energy absorption and scattering in polymers [16], [17]. Energy absorption is due to viscous effects, and scattering is due to inhomogeneities and internal boundaries. Attenuation also depends on sound wave frequency and is generally proportional to the square of the sound frequency [16], [18]. It is not possible to correlate calculated α values to a single frequency since we are dealing with blast waves with a frequency spectrum. The coefficients were determined by plotting $\ln(A/A_0)$ versus polymer thickness x and determining a linear least squares fit to the data points. The calculated amplitude attenuation coefficients are given in Table 3. Figure 11 plots the blast wave amplitude versus polymer

thickness using the calculated α values.

Table 3: Attenuation Coefficients

Material	Attenuation Coefficient (mm^{-1})
P1000	0.014
P650	0.013
P250/1000	0.014
Dragonshield-BC	0.067

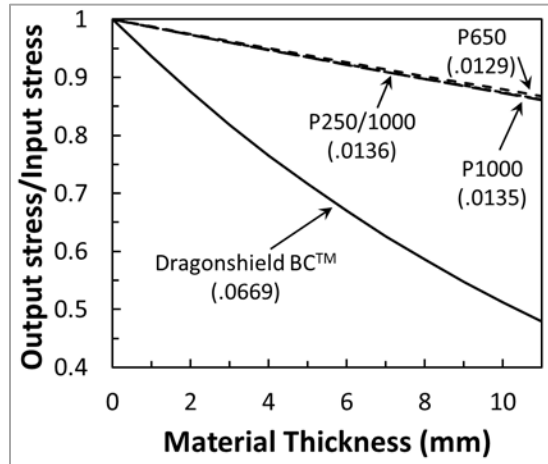


Figure 11: Blast Wave Amplitude versus Polymer Thickness

Flyer Plate Impact Experiments

Flyer plate impact experiments were conducted to determine dynamic material parameters for P250/1000 and Dragonshield-BC. Flyer plate impact experiments for P1000 and P650 were performed under another effort prior to this project [9]. Desired impact stresses were chosen based on these previous experiments and ranged from approximately 5–40 kbar (0.5–4 GPa) for the polyurea blend and 3–30 kbar (0.3–3 GPa) for Dragonshield-BC. The interface particle velocity, initial shock velocity, mean stress, and uniaxial strain were calculated for each experiment.

Experimental Setup

A metal impactor (9.5 mm thick by 31.8 mm diameter) was launched into a target sandwich configuration (35.6mm diameter) consisting of a polymer disc (6.5 mm thick) and two metal plates (0.8 mm thick on the polymer's impact side and 9.5 mm thick on the polymer non-impact side) as shown in Figure 12. For each experiment, all of the metal pieces were either 6061-T6 aluminum (density 2.691 g/cm^3 and a Rockwell B hardness of 60) or OFHC [oxygen-free high-thermal conductivity] half-hard copper (density 8.928 g/cm^3 and Rockwell F hardness of 79). A nominal 50 ohm manganin gauge, Dynasen's MN4-50-EFEP (3.8 x 3.8 mm active area), was placed on each side of the polymer disc. Gauge 1 was located on the front (impact side), and gauge 2 was located on the back (non-impact side). The front plate was needed to prevent gauge 1 from being destroyed prematurely on direct impact. Epoxy Technology Inc.'s EPO-TEK® 301 low-viscosity epoxy secured the gauges between the polymer and metal faces [13]. The average epoxy thickness was $9 \mu\text{m}$. The diameter of the impactor (31.8 mm) was less than the target diameter (35.5 mm) to ensure gauge 1 leads were protected from being cut prematurely by the edge of the impactor disc. Precision sabot and target preparation techniques minimized

impact tilt (less than 1 mrad).

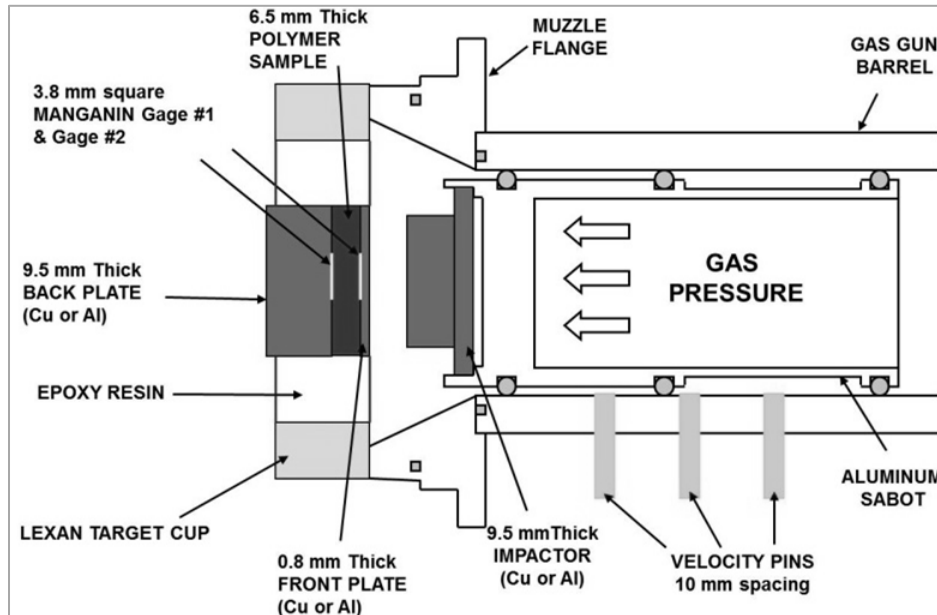


Figure 12: Flyer Plate Experiment Setup Cutaway

The target assembly was fixed to the muzzle as illustrated in Figure 13.

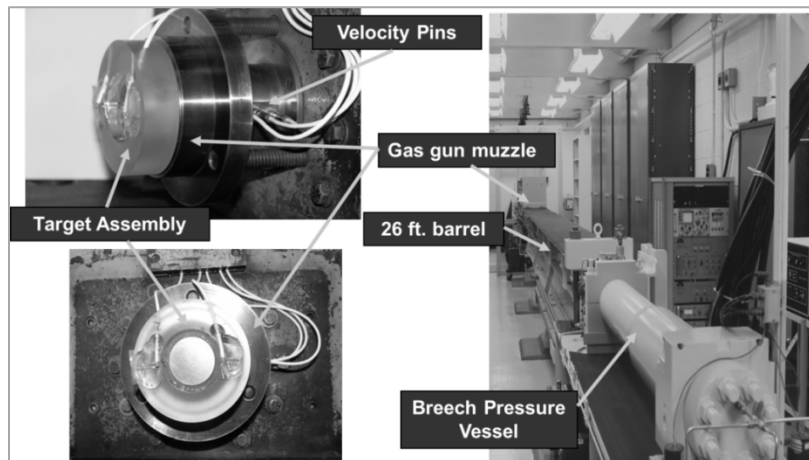


Figure 13: Flyer Plate Experiment Setup

Results and Discussion

Five impact experiments were performed on each of the two polymers at the velocities: 0.274, 0.366, 0.549, 0.762, and 0.914 mm/ μ s. These velocities correspond to impact stresses in the range of approximately 5–40 kbar (0.5–4 GPa) for the polyurea blend and 3–30 kbar (0.3–3 GPa) for Dragonshield-BC. The sabot velocity was measured just before impact to an error of less than 1% using three charged pins in the side of the barrel.

On impact, a shockwave moved into the front plate with a particle velocity equal to one half the impact velocity (symmetric impact). The metal impact stress was calculated using the known Hugoniot curves for either 6061-T6 aluminum [13] or OFHC half-hard copper [19]. The front

plate-polymer interface signal was measured with manganin gauge 1, and the polymer-back plate interface signal was measured with manganin gauge 2. A calibration curve was used to determine the stresses from the gauge signals (2–3% estimated uncertainty) [20]. Figure 14 shows the measured interface stresses for one of the shots, where impact occurs at 0 μs . Gauge 1 records the initial shock stress, and gauge 2 records the first re-shock stress. The shock transit times were determined from this data. The polymer longitudinal wave velocity U was calculated using $U = d/(\Delta t)$, where d is the measured polymer thickness and Δt is the shock transit time.

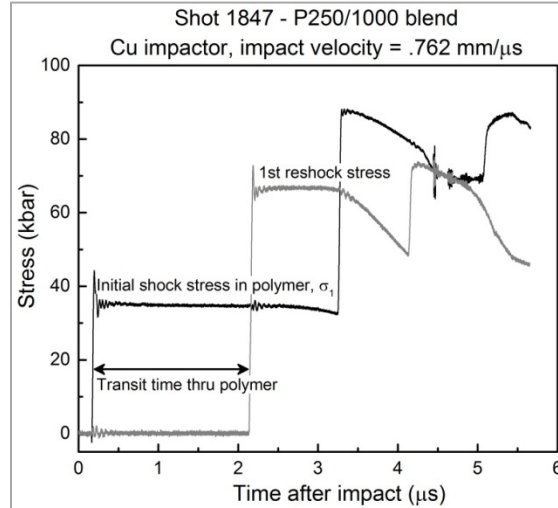


Figure 14: Manganin Gauge Results for Polyurea P250/1000 for Cu Disc Impact at 0.762mm/ μs

The interface particle velocities were determined using the measured interface stresses and the metal Hugoniot. Particle velocities calculated using the initial shock velocities in the momentum relation were 2–4% greater than those calculated using the measured interface stresses. The initial shock velocity in the polymer disc (1% estimated uncertainty) was determined by measuring the initial time difference (taken at the half-maximum gauge amplitude) between the gauge 1 (principal shock) and gauge 2 (first re-shock) signals. Figure 14 indicates that time-dependent effects for our impact conditions and time scale are minimal since the stress waves have sharp rise times and quickly reach a plateau that last for one or more microseconds.

Figure 15(a) and Figure 15(b) show the polymer wave velocity for each experiment and the average $U-u$ curve for the P250/1000 and Dragonshield-BC materials, respectively. The curves are a linear least squares fit to the data and are of the standard form $U = C_0 + su$, where C_0 and s are equation of state parameters for the polymer. The equation of state parameters C_B and C_L are also shown. These parameters were calculated in Phase 1 of this effort from the blast experimental data (see Figure 8) since these experiments occurred in the material's elastic region.

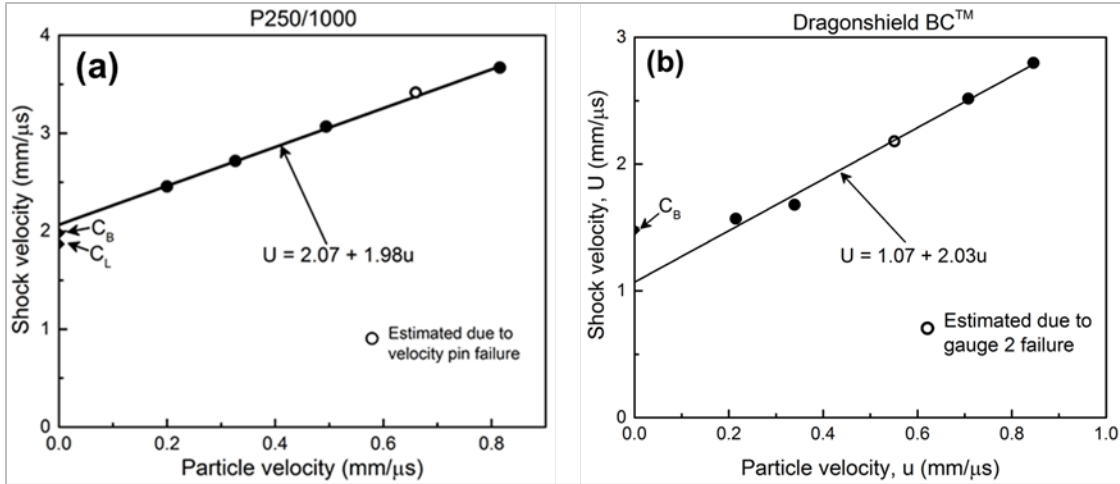


Figure 15: (a) P250/1000 $U-u$ Shock Properties (b) Dragonshield-BC $U-u$ Shock Properties

At 15 kbar, hysteresis effects become evident in the unloading behavior of the manganin gauge on the front of the sample. To account for this, the measured data points are corrected using a calibration curve, resulting in better agreement between the calculated and experimental outcomes. The corrected calculated stress-particle velocity points for each experiment are shown in Figure 16(a) and Figure 16(b) for P250/1000 and Dragonshield-BC, respectively. The curve fits for each polymer were determined by substituting $U = C_0 + su$ from Figure 15 into $\sigma = \rho_0 Uu$. The resulting curve is of the form $\sigma = \rho_0 C_0 u + \rho_0 s u^2$. The average polymer density was used for these calculations.

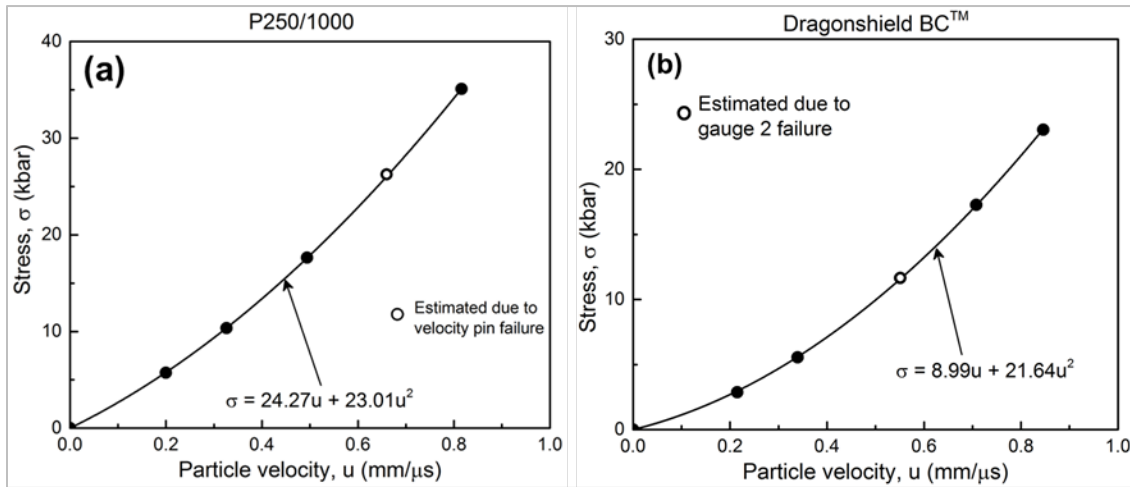


Figure 16: (a) P250/1000 $\sigma-u$ Shock Properties (b) Dragonshield-BC $\sigma-u$ Shock Properties

The experimental results are summarized in Table 4 and Table 5, where the shock velocities are in laboratory coordinates. The initial polyurea P250/1000 stresses vary from 5.7–34.8 kbar, and Dragonshield-BC stresses vary from 2.9–23.0 kbar.

Table 4: Polyurea P250/1000 Principal Hugoniot Experimental Results

P250/1000 Blend	Experiment No.				
	1	2	3	4	5
Impactor, front and back plate material	6061-T6 Al	OFHC half-hard Cu	OFHC half-hard Cu	OFHC half-hard Cu	OFHC half-hard Cu
Impact velocity (m/ μ s)	0.26	0.37	0.55	0.75	0.92
Shock velocity, U (mm/ μ s)	2.46	2.72	3.07	3.42	3.67
Particle velocity, u (mm/ μ s)	0.20	0.33	0.49	0.67	0.82
Mean stress, σ (kbar)	5.47	10.3	17.6	26.7	34.8
Uniaxial strain, $\varepsilon = u/U$	0.08	0.12	0.16	0.20	0.22

Table 5: Dragonshield-BC Principal Hugoniot Experimental Results

Dragonshield-BC	Experiment No.				
	1	2	3	4	5
Impactor, front and back plate material	6061-T6 Al	OFHC half-hard Cu	OFHC half-hard Cu	OFHC half-hard Cu	OFHC half-hard Cu
Impact velocity (mm/ μ s)	0.26	0.36	0.55	0.77	0.92
Shock velocity, U (mm/ μ s)	1.57	1.68	2.18	2.52	2.80
Particle velocity, u (mm/ μ s)	0.22	0.34	0.55	0.71	0.85
Mean stress, σ (kbar)	2.9	5.6	11.7	17.3	23.0
Uniaxial strain, $\varepsilon = u/U$	0.14	0.20	0.25	0.28	0.30

Phase 1 Conclusion

Blast Wave Experiments

Twenty-eight air blast wave experiments in the stress range 0.5–2 bar were conducted on four polymer materials: P1000, P650, P250/1000 blend, and Dragonshield-BC. 6061-T6 aluminum calibration experiments and CTH simulations validated the PVDF stress gauges. Polymer $U-u$, $\sigma-u$, and $\sigma-\varepsilon$ equations were determined. Impedance-matching techniques calculated polymer input and output stress and blast attenuation. Polymer attenuation increased

with material thickness. The attenuations for the P1000, P650, and P250/1000 blend were similar, and significantly less than the Dragonshield-BC attenuation. NUWCDIVNPT used these material parameters for computational model development and validation to investigate in detail the influence of specific parameters on polymer performance against blast.

Flyer Plate Impact Experiments

A total of ten flyer plate impact experiments were conducted to determine dynamic material parameters for P250/1000 and Dragonshield-BC. Five velocities—0.274, 0.366, 0.549, 0.762, and 0.914 mm/ μ s—were chosen based on the stresses from previous P1000 and P650 experiments performed under another effort. The interface particle velocity, initial shock velocity, mean stress, and uniaxial strain were calculated for each experiment. The initial stresses in polyurea P250/1000 varied from 5.7–34.8 kbar, and the Dragonshield-BC stresses varied from 2.9–23.0 kbar. NUWCDIVNPT will use these material parameters for computational model development and validation to investigate in detail the influence of specific parameters on polymer performance against impact.

PHASE 2

Materials

Kevlar fabric was procured based on Paul Cavallaro's recommendation and chosen to match the materials investigated by NUWCDIVNPT in its previous series of experiments. Three weave styles were chosen: plain; 2 \times 2 twill; and 4H satin weaves with Kevlar KM2 Plus fiber (a high-performance para-aramid developed for use in military body armor vests and helmets). The weave styles, shown in Figure 17, were obtained in the greige (untreated) state. Plain weave is the most common and tightest weave structure in which one weft thread passes over and under one warp thread. In a twill (2 \times 2) weave, two weft threads cross two warp threads. In satin a (4H) weave, four weft threads cross four warp threads. The mechanical properties of the yarns are listed in Table 6.

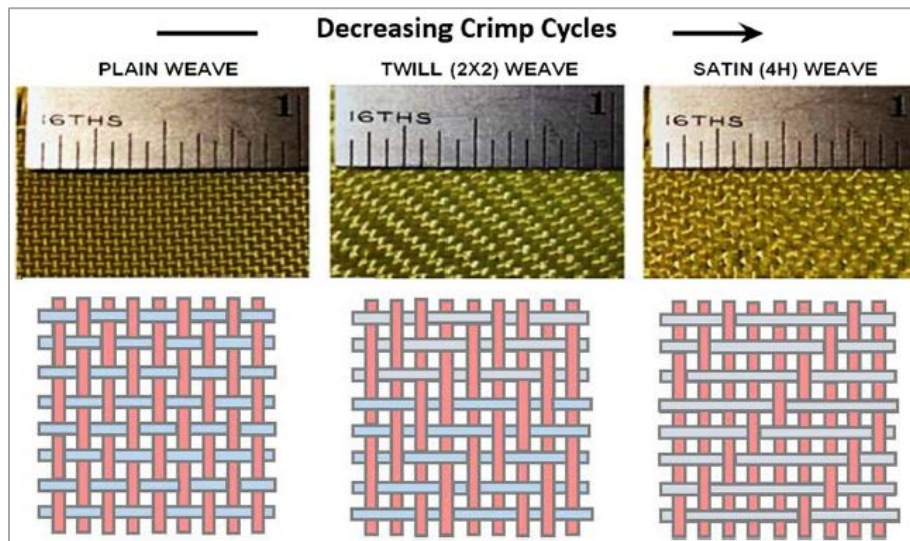


Figure 17: Kevlar Weave Styles

Table 6: Nominal Mechanical Properties of Kevlar KM2 Plus Yarns

Property	Value
Linear Density	600 denier
Tenacity	28.4 gpd
Breaking Strength	166.8 Newton
Elongation at Break	3.8%
Elastic Modulus	660.0 gpd

Denier is the mass in grams of 900m of yarn. Yarn tenacity and elastic modulus are defined in terms of grams per denier (gpd).

Additional data describing the fabric weave styles and crimp contents are provided in Table 7. C_{warp} and C_{weft} are the warp and weft crimp percentage contents, and ξ is the crimp ratio C_{warp}/C_{weft} [20]. In weaving a fabric, warp is a term that defines the yarn that is held stationary in tension on the loom and weft is the longitudinal yarn that is drawn over and under the warp. The yarn crimp percentage is the ratio of the yarn straight length less the length in the fabric and the length of the fabric, expressed as a percentage.

Table 7: Kevlar KM2 Plus Fabric Weave Styles and Properties

Weave Style	Plain	Twill 2x2	Satin 4H
Yarn denier (warp/weft)	600/600	600/600	600/600
Warp/weft counts (yarns/10cm)	122x122	122x122	122x122
Areal density (g/m ²)	163.4	163.1	163.8
Fabric thickness (mm)	0.22	0.20	0.21
C_{warp} (%)	1.6	1.2	1.2
C_{weft} (%)	1.6	1.2	1.2
ξ	1.0	1.0	1.0
Fabric state	Greige	Greige	Greige

Three different laminate panels, each containing 20 layers of fabric, were manufactured by Core Composites Corporation, a division of Core Molding Technologies Inc. The first panel was constructed of plain weave fabric. The second panel was constructed of twill weave fabric. The third panel was a hybrid panel constructed with layers of the three weave styles arranged in a crimp gradient (CG) manner as 3-Plain/4-Twill/3-Satin. The fabrics were stacked with consistent alignment of the warp and weft axes. A room-temperature, wet layup compression molding process was used with a thermoset epoxy resin. Mechanical stops were employed in the mold to achieve approximate fiber volume fractions of 47–50 % for each laminate.

Experimental Setup

Using a waterjet, the laminate Kevlar panels were cut into discs of approximately 34.5 mm diameter. Table 8 lists sample dimensions. The sample discs were fixed in a sabot and launched using the gas gun into a target assembly holding a 3.175 mm, 0.1237 g steel sphere attached to the muzzle.

Table 8: Kevlar Sample Dimensions

Shot	Weave Pattern	Mass (g)	Average Thickness (mm)	Average Diameter (mm)	Density (g/cm ³)	Areal Density (g/cm ²)
1873	Plain	4.3813	4.337	34.531	1.0787	0.4678
1874	Plain	4.4991	4.304	34.709	1.1048	0.4755
1875	Plain	4.4368	4.349	34.595	1.0854	0.4720
1876	Plain	4.3435	4.290	34.601	1.0767	0.4619
1877	Plain	4.3630	4.297	34.430	1.0907	0.4686
1878	Plain	4.2173	4.351	34.404	1.0427	0.4536
1879	Twill	4.7376	4.241	34.595	1.1884	0.5040
1880	Twill	4.7990	4.239	34.557	1.2070	0.5117
1881	Twill	4.8788	4.209	34.538	1.2372	0.5208
1882	Twill	4.7316	4.283	34.506	1.1814	0.5060
1883	Twill	4.6981	4.215	34.569	1.1874	0.5006
1884	Hybrid	4.6351	4.221	34.569	1.1698	0.4938
1885	Hybrid	4.6206	4.178	34.436	1.1875	0.4961
1886	Hybrid	4.7088	4.201	34.455	1.2023	0.5050

The sabot assembly consists of a series of aluminum discs and rings shown in Figure 18. The front plate is 6.35 mm thick aluminum with a 6.35 mm diameter hole in the center and was used to prevent the rags in the soft recovery box from causing further sample deformation. After the front plate is a 6.35 mm long, 34.036 mm outside diameter aluminum spacer ring with a 2.6924 mm wall thickness that prevents deformation of the front aluminum plate due to rags impacting the sample. The sample follows, and a fragment soft recovery assembly made up of an aluminum spacer with three 2-120 Parker-Hannifin Corp.TM Parker® O-rings followed by three 3.429 mm-thick rubber discs secured with a 5-minute epoxy comes next. The final disc is a 3.175 mm-thick aluminum pusher disc secured with a layer of Kurt J. Lesker Company® Torr Seal® and five-minute epoxy.

Figure 18 shows the target assembly consists of three Sabic Global Technologies B.V. LexanTM rings with paper and DuPontTM Mylar® discs dividing them. The first Lexan ring (attached to the muzzle) is 12.7 mm thick. It is followed by a 0.1016 mm paper disc with a 2.54 mm hole punched in the center for the 3.175 mm steel sphere to sit in, as well as four other holes approximately 5.08 mm in diameter to allow vacuum to leak through. The next piece was a Lexan 19.05 mm-thick alignment ring with a raised edge on both sides for the other discs to fit into. A piece of 0.1143 mm thick Mylar, enabling the barrel to be evacuated, fits between the alignment ring and 6.35 mm-thick back ring.

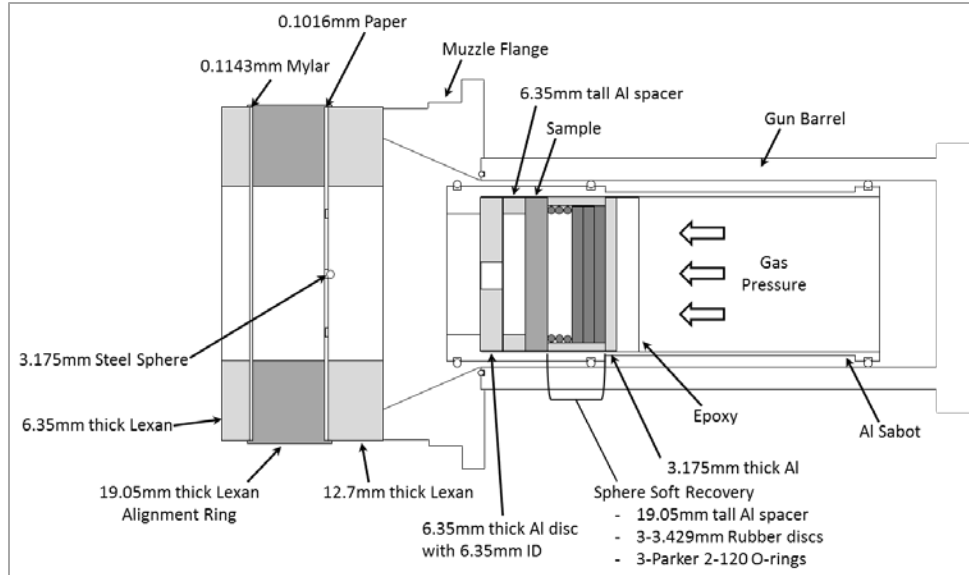


Figure 18: Target and Sabot Assembly Cutaway

Results and Discussion

A series of 12 experiments for three layered composite panels was conducted to evaluate the effect of composite weave style on penetration threshold. To do this, the minimum velocity required to perforate the material was determined for each panel. The sabot velocity was measured just before impact to an error of less than 1% using three charged pins in the side of the barrel. Due to the limited amount of material, checkout shots were conducted using discs from a similar Kevlar panel leftover from a previous experimental program. The velocity found to be the penetration threshold for this Kevlar was used as the starting velocity for the plain weave experiments. After each experiment, based on whether or not the material was perforated, the velocity was adjusted to hone in on the threshold until it was within 15 m/s. This was done by splitting the difference between the velocities of the two previous experiments. When the penetration threshold for the sample was found, a repeat experiment was conducted to ensure repeatability. When moving to the next material, twill weave, the plain weave penetration threshold was used as the starting velocity. This same method was used throughout the experimental series. Table 9 lists the impact velocity and whether or not the sample was perforated. The experiments with velocities just above and below the penetration threshold are highlighted, and the results from these experiments are shown in Figures 19–24.

Table 9: Kevlar Penetration Threshold Results

Shot	Weave Pattern	Actual Velocity (m/s)	Perforated Sample (Y/N)
1875	Plain	434.2	No
1876	Plain	458.7	No
1877	Plain	466.4	No
1878	Plain	474.1	Yes
1874	Plain	483.6	Yes
1873	Plain	562.0	Yes
1879	Twill	469.6	No
1881	Twill	507.5	No
1883	Twill	515.1	Yes
1882	Twill	519.3	Yes
1880	Twill	535.8	Yes
1885	Hybrid	506.3	No
1884	Hybrid	517.1	Yes
1886	Hybrid	519.5	Yes

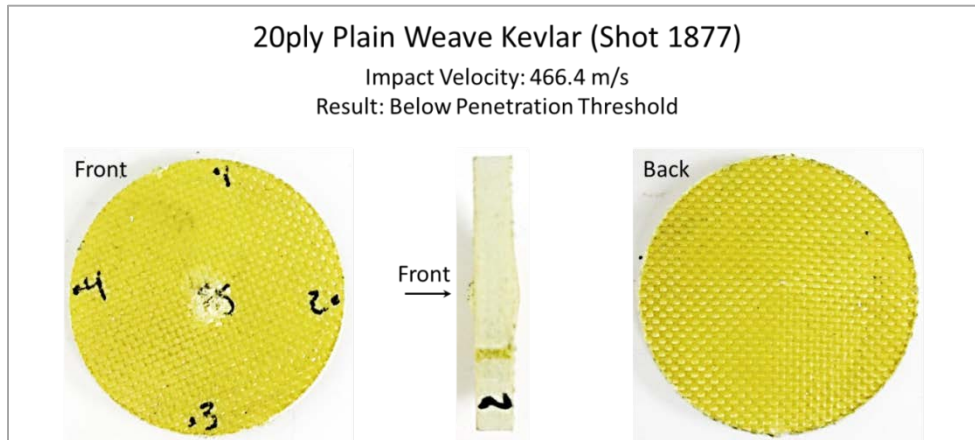


Figure 19: Plain Weave Kevlar below Penetration Threshold Result



Figure 20: Twill Weave Kevlar below Penetration Threshold Result



Figure 21: Hybrid Weave Kevlar below Penetration Threshold Result

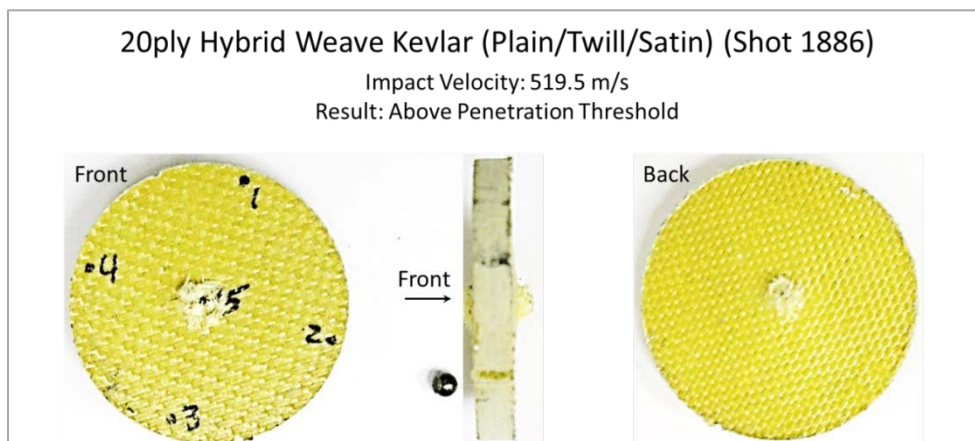


Figure 22: Hybrid Weave Kevlar above Penetration Threshold Result

Phase 2 Conclusions

A series of 12 reverse ballistics impact experiments for three layered composite panels (plain weave, twill weave, and hybrid (plain/twill/satin)) was conducted to evaluate the effect of composite weave style on penetration threshold. The penetration threshold velocity was determined as the minimum velocity within 15 m/s required to perforate the sample material.

The penetration thresholds for the panels were determined to be the following: 472.4 m/s for the plain weave and 518.2 m/s for both the twill and hybrid weaves. For our experiments, these results suggest that the weave pattern and composite areal density influence the penetration threshold velocity. The average areal densities from Table 8 are 0.467, 0.509, and 0.498 g/cm² for the plain weave, twill weave, and hybrid weave, respectively. NUWC DIVNPT will use the results from this experimental series to compare with results from a previous study the center conducted.

REFERENCES

- [1] W. H. Holt and W. J. Mock, "The NSWC Gas Gun Facility for Shock Effects in Materials," Naval Surface Warfare Center, Dahlgren Division, 1976.
- [2] W. H. Holt and W. J. Mock, "Computation of Fragment Mass Distributions for HF-1 Steel Explosive-filled Cylinders," *Journal of Applied Physics*, vol. 58, no. 3, p. 1223–1228, August 1985.
- [3] T. El Sayed, W. J. Mock, A. Mota, F. Fraternali and M. Ortiz, "Computational assessment of ballistic impact on a high strength structural steel/polyurea composite plate," *Computational Mechanics*, vol. 43, no. 4, p. 525–534, March 2009.
- [4] W. J. Mock and W. H. Holt, "Technique for Measuring the Ballistic-Limit Velocity for Small Mass Fragments Impacting Thin Metal Plates," *Review of Scientific Instruments*, vol. 72, no. 10, p. 3975–3978, October 2001.
- [5] X. Liang, W. J. Mock and T. Belytschko, "Penetration of DH-36 Steel Plates With and Without Polyurea Coatings," *Mechanics of Materials*, vol. 42, no. 11, p. 981–1003, November 2010.
- [6] W. J. Mock and J. Drotar, "Effect of Aluminum Particle Size on the Impact Initiation of Pressed PTFE/AL Composite Rods," in *AIP Conference Proceedings 955*, 2007.
- [7] W. J. Mock and W. H. Holt, "Reactive munition in a three dimensionally rigid state". United States Patent 7383775, 10 June 2008.
- [8] W. H. Holt, W. J. Mock, F. Santiago and R. M. Gamache, "Experiment to Capture Gaseous Products from Shock-decomposed Materials," in *AIP Conference Proceedings 620*, 2002.
- [9] W. J. Mock and W. H. Holt, "Pulse Charging of Nanofarad Capacitors from the Shock Depoling of PZT 56/44 and PZT 95/5 Ferroelectric Ceramics," *Journal of Applied Physics*, vol. 49, no. 12, p. 5846–5854, December 1978.
- [10] W. J. Mock, S. Bartyczak, G. Lee, J. Fedderly and K. Jordan, "Dynamic Properties of Polyurea 1000," in *16th APS Topical Conference on Shock Compression of Condensed Matter*, Nashville, Tennessee, 2009.
- [11] E. Balizer, J. Fedderly, G. Lee and S. Bartyczak, "Investigation of Microstructural Changes in Impacted Polyurea Coatings Using Small Angle X-Ray Scattering," *Powder Diffraction*, vol. 26, no. 2, p. 149–154, 2 June 2011.
- [12] S. Bartyczak and W. J. Mock, "Versatile Gas Gun Target Assembly for Studying Blast Wave Mitigation in Materials," in *Shock Compression of Condensed Matter—2011: Proceedings of the Conference of the American Physical Society Topical Group on Shock Compression of Condensed Matter*, Chicago, Illinois, 2011.
- [13] D. R. Christman, W. M. Isbell, S. G. Babcock, A. R. McMillan and S. J. Green, "Measurements of Dynamic Properties of Materials Volume III: 6061-T6 Aluminum," General Motors Corporation, Warren, Michigan, 1971.
- [14] NDT Education Resource Center, "Attenuation of Sound Waves," [Online]. Available: <https://www.nde-ed.org/EducationResources/CommunityCollege/Ultrasonics/Physics/attenuation.htm>. [Accessed 5 January 2018].
- [15] W. E. Baker, *Explosions in Air*, University of Texas Press, 1973, p. 285.
- [16] A. Garbacz and E. J. Garbozi, "Ultrasonic Evaluation Methods Applicable to Polymer Concrete Composites," National Institute of Standards and Technology, Gaithersburg, Maryland, 2003.

- [17] J. Jarzynski, "Mechanisms of Sound Attenuation in Materials," in *Sound and Vibration Damping with Polymers*, 1990.
- [18] J. W. S. Rayleigh, *The Theory of Sound*, Vol 2, Second ed., New York, New York: Dover Publications, 1945, p. 544.
- [19] Z. Rosenberg, D. Yaziv and Y. Partom, "Calibration of Foil-like Manganin Gauges in Planar Shockwave Experiments," *Journal of Applied Physics*, vol. 51, no. 7, p. 3702–3705, 1 July 1980.
- [20] P. V. Cavallaro, "Effects of Weave Styles and Crimp Gradients in Woven Kevlar/Epoxy Composites," *Experimental Mechanics*, vol. 56, no. 4, p. 617–635, April 2016.

DISTRIBUTION

	Copies	
	Hard	Soft
DOD ACTIVITIES (CONUS)		
DEFENSE TECH INFORMATION CTR 8725 JOHN J KINGMAN RD SUITE 0944 FORT BELVOIR, VA 22060-6218	0	1
NON-DOD ACTIVITIES		
THE CNA CORPORATION ATTN DOCUMENT CENTER 3003 WASHINGTON BOULEVARD ARLINGTON VA 22201	0	1
INTERNAL		
1033 (NSWCDD TECHNICAL LIBRARY)	1	1
H	0	1
H30	0	1
H32	0	1
H32 (BARTYCZAK)	4	1
H32 (DOHMEIER)	0	1
H32 (EDGERTON)	1	1
H32 (MOCK)	0	1
H09 (PARKER)	0	1

